ENCIT 2018

ABCM Associação Brasileira de Engenharia e Ciências Mecânicas

17th Brazilian Congress of Thermal Sciences and Engineering
November 25th-28th, 2018, Águas de Lindóia, SP, Brazil

ENCIT-2018-0099
SOOT DISTRIBUTION IN TURBULENT BLUFF BODY NEAR WAKE NON PREMIXED FLAMES

Suzane Pereira dos S. Nascimento
Juan José Cruz Villanueva
Luís Fernando Figueira Silva
Pontifícia Universidade Católica do Rio de Janeiro, Department of Mechanical Engineering, Rio de Janeiro, Brazil
pereirasu@outlook.com.br
luisfer@puc-rio.br

Abstract. *Combustion has been the foundation of worldwide industrial development for the past 200 years. In particular, industry relies heavily on the combustion process. The major uses for combustion in industry are oil and natural gas production, solution heat treating. A major concern has always been improving the energy efficiency of industrial combustion processes, however, this has shifted towards pollution emissions, such as soot. Studies on turbulent sooting flames that are similar to those found in the industrial burners are required to improve the knowledge which is a prerequisite to developing new processes. In this work, ethylene/air and methane/air turbulent flames stabilized on the near wake of a bluff body type burner are characterized by means of light extinction and laser induced incandescence techniques. This allow to measure the soot volume fraction and soot planar distribution of the studied flames. The obtained results indicate that the methane/air flames produce an order of magnitude less soot than the corresponding ethylene/air ones. Significant turbulent soot intermittency is observed, which is associated to highly distorted flame structures. Results obtained with delayed and prompt signal detection could lead to identifying the presence of polycyclic aromatic hydrocarbons.*

Keywords: *Laser extinction, Laser induced incandescence, Turbulent flames, Soot*

1. INTRODUCTION

Environmental protection is becoming an important socio-economic issue nowadays. Environmental quality and greenhouse gases are seen as some of the key drivers shaping the future of energy and industrial combustion. Around the world, environmental protection awareness is increasing, with stricter laws in recent years regulating acceptable levels of ambient air pollution. On the other hand, the number of vehicles, power plants and factories in operation is also increasing (Sun *et al.*, 2016). Energy demand and its consumption are growing annually, forcing power plants to produce more electrical and heat energy, which is connected with large volumes of pollution gases (Chmielewski, 2013). Studies have shown that air pollution is a major cause of cardiovascular diseases and endothelial dysfunction. It has also been shown that exposure to air pollution and traffic from major highways is associated with a high risk of atherosclerosis, such as that shown by premature aortic and coronary calcification (Bourdrel *et al.*, 2017). Therefore, the enhanced understanding of combustion processes is fundamental to a better comprehension of how energy efficiency can be achieved simultaneously with health environmental impacts reduction.

In this context, improving the knowledge about combustion phenomena by the application of laser diagnostics techniques should contribute to the development of more efficient combustion devices, with an associated pollutants emission reduction (Franzelli *et al.*, 2015). The aim of this work is to explore the potential of laser techniques to characterize soot distribution in non premixed turbulent ethylene/air and methane/air flames stabilized in a bluff body type burner near wake region. These flames are examined using light extinction, in order to quantify the averaged integral soot volume fraction, and with laser induced incandescence (LII) technique, so as to provide the instantaneous soot distribution.

Classically, different laminar flames are applied in the study of soot formation, selected accordingly to the kind of phenomena to be studied and stabilized in different type of burners. Gulder *et al.* (2006) report studies performed in a co-flow ethylene/air diffusion flame with an axi-symmetric configuration; this kind of flame is very useful to calibrate LII technique. Axelsson *et al.* (2000) use a Mckenna burner to calibrate flame temperature measurements, to perform flame speed measurements, and to characterize of soot formation using the LII technique. Quay *et al.* (1994) explore the LII technique to measure two-dimensional soot volume fraction distribution, f_v, in an ethylene/air laminar hyperventilated co-flow flame. The results allow to eliminate many of the limitations associated to the f_v measurements obtained by laser extinction, such as tomographic inversion of a integral measurements group through the beam optical path.

The turbulent flames stabilized in bluff body burners exhibit complex flows, involving recirculation zones similar

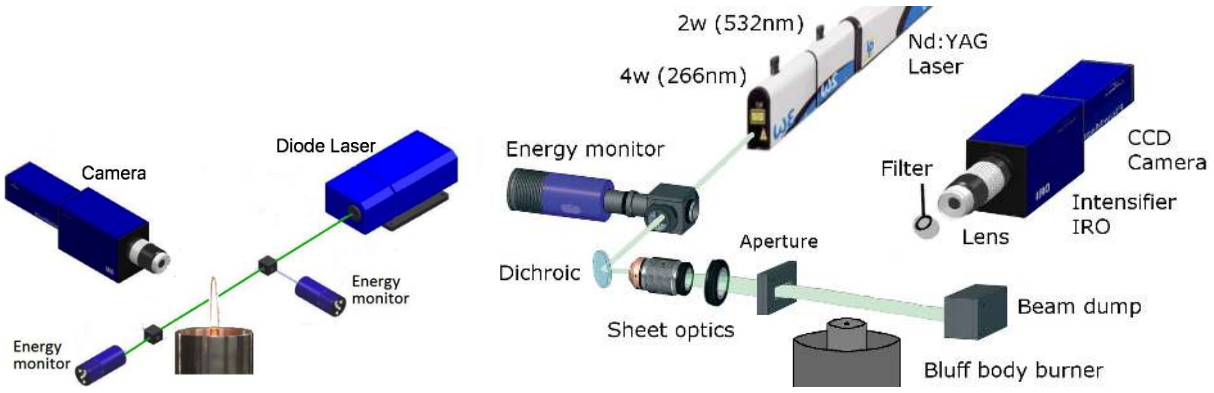

(a) Light extinction.

(b) Laser induced incandescence.

Figure 1: Experimental setup schemes.

to those found in the industrial burners. Two vortexes are found in the recirculation zone, an exterior one near the air stream, and an interior vortex, closer to the fuel jet (Dally *et al.*, 1998a). In this type of burner, the rate of air and fuel flow may be varied and the interaction between the chemical process and the turbulence can be studied in different combustion regimes (Huang and Lin, 1994; Dally *et al.*, 1998b; Esquiva-Dano *et al.*, 2001; Dawson *et al.*, 2011; Caetano and Figueira da Silva, 2015). Previous studies (Cruz Villanueva and Figueira da Silva, 2016) discussed the measured averaged velocity and turbulence fields in a situation when the air annular flow is present only. The velocity and OH fluorescence radical distribution in several methane/air flame regimes has also been addressed (Caetano and Figueira da Silva, 2015).

The paper is organized as follows. In section 2, the methodology is presented with an overview of the burner and optical techniques used to measure the soot volume fraction and soot planar distribution. The results are presented in section 3, where the influence of turbulence in soot formation and distribution is discussed. In section 4 the main findings are summarized and perspectives are given.

2. EXPERIMENTAL METHODOLOGY

2.1 Bluff Body Burner

The non premixed bluff body burner characteristics have been described in detail in previous studies (Caetano and Figueira da Silva, 2015; Cruz Villanueva and Figueira da Silva, 2016). In the present work the central fuel jet tube diameter (D_j) has been reduced to 4.3 mm, while maintaining the same bluff body diameter, $D_b = 60$ mm. The bluff body is surrounded by a concentric 200 mm diameter tube which provides the air co-flow. The bluff body vertical alignment is carefully set by precision screws located at the base, where is located a perforated disc with 12 mm holes to ensure uniform flow and turbulence level. The bluff body surface lies 30 mm above the exit plane of annular air tube, in order to provide ample optical access, allowing for easy application of optical diagnostics.

Annular air flow is fed by a centrifugal fan, Deltra VC-400, that leads to a maximum air velocity $U_a = 11.8$ m/s, and thus to a bluff body diameter based Reynolds number of $Re_b = 45,400$. A mass flow meter, Bronkhorst EL-FLOW F-201AC-AAA-33-V, with a 0.8%. maximum reading uncertainty is used to control the fuel flow rate. In this work are used the values of 2.50 lpm for methane and 1.97 lpm for ethylene.

2.2 Laser Extinction Technique

The laser extinction technique, which setup is shown in Fig.1a, is applied for soot volume fraction measurements. A CW diode laser (DPSS - LaVision) with 532 nm wavelength, 0.5 W of nominal power, laser beam diameter of 330 μm, is used as light source. Two energy monitors (V9- LaVision, with a detector integration time of 1.5 ms) measure the laser intensity before, I_0, and after, I, passing through the probed flame. The flame natural emission is captured with a camera (Canon Rebel T3E) with an exposure time of 1/200 s.

A review of the light extinction technique and its relation with the soot volume fraction is given by Zhao and Ladommatos (1998). The Beer-Lambert law refers to the optical properties of the attenuating medium and the intensities of the collimated beam before, $I_\lambda(0)$, and after, $I_\lambda(L)$, of this medium resulting in:

$$\frac{I_\lambda(L)}{I_\lambda(0)} = \tau = \exp\left(-\frac{\int_0^L K_\lambda f_v \mathrm{d}l}{\lambda_{det}}\right), \tag{1}$$

where τ represents the transmittance of the laser beam in the participating medium, K_λ is the dimensionless extinction coefficient given by $K_\lambda = 6\pi E(m)$, where E(m) = 0.245 is the soot absorption function (Chang and Charalampopoulos (1990)), L ($\approx$ 60 mm) the optical path along the flame and λ_{det} is the wavelength used (532 nm). Using the simplifying hypothesis that the dimensionless extinction coefficient K_λ is constant along the optical path, L, the extinction technique allows to calculate an average value, $\bar{f_v}$, from the integrated value of the soot volume fraction, $\bar{f_v}$L = $F_v = \int_0^L f_v \mathrm{d}l$ as (Modest (2013)):

$$\bar{f_v} = -\frac{\lambda}{K_\lambda L} ln(\tau), \tag{2}$$

the measured $\bar{f_v}$ could be used to calibrate the qualitative LII results if the optical path, L, is superimposed on the laser induced incandescence sheet used.

The use of the light extinction technique for the analysis of turbulent combustion requires special attention because, in addition to the spatial interaction, Eq. 1, a temporal integration is also carried out during which the flame fluctuates. With this, the luminous intensity measured is a function of time, I_λ (L, t). In order to account for this double integration, the following intensities are defined:

$$I_\lambda\ (L,T) = \frac{1}{T}\int_0^T I_\lambda(L,t)\mathrm{d}t$$
$$I_\lambda\ (0,T) = \frac{1}{T}\int_0^T I_\lambda(0,t)\mathrm{d}t$$

where T is the integration time of the detector. In the case of turbulent flames, an average transmittance is then measured:

$$\bar{\tau} = \frac{I_\lambda(L,T)}{I_\lambda(0,T)} = \frac{1}{T}\int_0^T exp(-\int_0^L k_\lambda \mathrm{d}l). \tag{3}$$

In the present study it should be recognized that $\bar{f_v}$ (L, T) is a stochastic quantity; due to the turbulent fluctuations of the flame, influencing k_λ e and L. As will be seen further, the comparison between the value of T and that of the time scales of the turbulent motion determines the physical significance of $\bar{f_v}$ (L, T) that can be calculated with Eq. 2.

2.3 Laser Induced Incandescence Technique

The LII technique setup is shown in Fig. 1b. For simultaneous polycyclic aromatic hydrocarbons (PAH) fluorescence and soot incandescence, the excitation is performed with the 4^{th} harmonic (266 nm) of a Brilliant b (Quantel) Nd:YAG laser, with 80 mJ nominal energy, and operated at 10 Hz (Vander Wal, 1996; Vander Wal *et al.*, 1997; de Andrade Oliveira *et al.*, 2013). A dichroic mirror is used to filter the second harmonic (532 nm) residual component. The shot-to-shot energy fluctuation of laser is measured by an energy monitor (LaVision), in order to reject measurements obtained beyond a standard deviation of the beam mean energy. A thin planar sheet of 0.45×35 mm^2, vertically dislocated 10 mm above bluff body face, and that passes through the symmetry plane of the burner, is generated using two pairs of lenses. The first two are spherical lenses, $f = -80$ mm and 100 mm, that converge the beam to the desired thickness, whereas the second pair of cylindrical lenses, $f = -50$ mm and 150 mm, vertically expands the beam. The LII signal has been measured as a function of the laser fluence in a laminar flame (Cruz Villanueva and Figueira da Silva, 2017) and the so-called plateau region is observed beyond 0.08 J/cm^2. Accordingly, this laser fluence value is supposed to represent the present experimental situation.

The incandescence signal is captured perpendicular to the laser sheet by a CCD camera (Imager Intense, LaVision) with 1376×1040 pixels, coupled to an intensifier (Intensifier Relay Optics, LaVision) equipped with a P43 photosensor. A lens $f/2.8$-100 mm (UV lens enhanced, LaVision) with filters centered at 340 and 400 nm, 10 nm bandwidth and 90% of transmissivity, are used to perform soot and PAH spectral characterization.

The corresponding measurements resolution is 16 px/mm. In order to avoid the polycyclic aromatic hydrocarbon (PAH) fluorescence, a delayed detection of 50 ns with respect to laser pulse and an intensifier gate of 20 ns are used, so as to capture soot incandescence only. These results are compared with prompt detection (0 ns) in order to evaluate the PAH + soot distribution. For each experimental condition, a set of $4,000$ images is acquired and post-processed by applying background subtraction, energy shot-to-shot fluctuation and laser sheet correction (Qamar *et al.*, 2009; Cruz Villanueva and Figueira da Silva, 2017).

3. RESULTS AND DISCUSSIONS

In this section the average ethylene/air sooting flame structure and the measured soot volume fraction are first presented. Then, is given a detailed characterization of soot volume fraction and polycyclic aromatic hydrocarbons fluorescence at two different wavelengths, 340 and 400 nm.

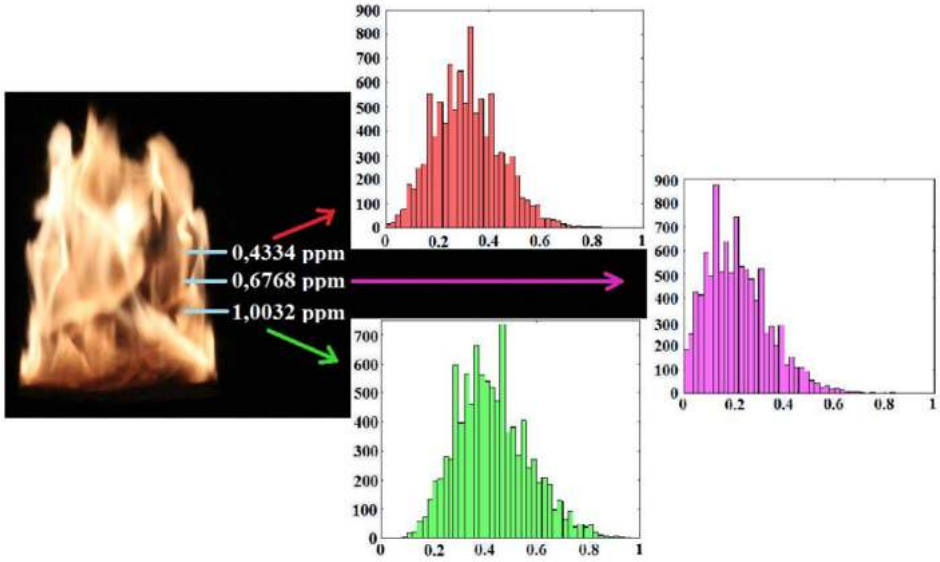

Figure 2: Soot volume fraction for different vertical positions (27, 37 and 47 mm above the burner surface) at the bluff body burner centerline, also shown are the extinction histogram at these positions.

The measurements have been carried out with flow rates of 1.97 Nlpm for ethylene, and 2.50 Nlpm for methane. The corresponding fuel jet Reynolds number, Re_j, are 1,070 and 720 for ethylene methane, respectively. Therefore, the flow in the fuel feed tube is expected to be laminar. However, upon the interaction with the recirculation zone, turbulent conditions are achieved, and the turbulent state of the recirculation zone is expected to be controlled by the air flow. The co-flow air velocity used is 11.8 m/s at 1 bar, resulting on a Reynolds number of $45,400$. The maximum measured soot volume fraction is 1.0 ppm for ethylene/air and 0.02 ppm for methane/air flames.

3.1 Sooting Flame Structure and Soot Volume Fraction

The ethylene/air turbulent sooting flame structure may be observed in the photograph of Fig. 2. The corresponding histogram of the flame extinction $\bar{\tau}$ shows a monomial distribution behavior with the highest value of soot volume fraction found in the lowest part of the flame. The stochastic behavior of $\bar{f_v}$ may be understood by considering the values of detection and turbulence time scales. Indeed, the depicted results have been obtained with a detection time of $T = 1.5\,ms$, which is of the same order of magnitude as the estimated turbulence integral scale, $t_0 = 1.27\,ms$. Therefore, the histograms indicate $\bar{f_v}$ excursions which have time scales comparable to the largest turbulence motions. Therefore, it should be stressed that small scale turbulence fluctuations are not resolved. A note that to has been estimated using measured values of the turbulent kinetic energy (Cruz Villanueva and Figueira da Silva, 2016).

The turbulent nature of the flame is underscored by the extinction distribution. Indeed, at some of the heights along the flame a non-negligible zero extinction probability is observed. On the contrary, at the lowest measurement height almost complete extinction is often found to occur. This may be explained both by a high flame soot loading and by a frequent change of the optical path thickness responsible for laser attenuation. Note that obtaining an instantaneous value of soot volumetric fraction from such laser extinction data would require the combined knowledge of the instantaneous optical path, which is not available, and a strong hypothesis involving the medium homogeneity along the laser path.

As it may be seen in the histograms given in Fig. 3, the methane/air flame has a significantly smaller soot volume fraction – approximately an order of magnitude less – when compared with the ethylene/air flame. Indeed, ethylene is known for producing a sooting flame, has a considerable degree of extinction in laminar diffusion flames (Gulder *et al.*, 2006). This is the reason why further extinction or LII measurements have not been attempted for the methane/air flames.

3.2 Planar Soot Distribution

The instantaneous 400 nm delayed and prompt fields and 340 nm prompt field are shown in Fig. 4 for the studied ethylene/air flame. Here, the intermittence index, $\Omega(x, y)$, is defined as the fraction of measurements where a non-zero signal is observed (Lee *et al.*, 2009). In the present study Ω is calculated by averaging the binarized fields, after using a threshold above the characteristic ICCD image noise.

The instantaneous fields given in Fig. 4 are significantly different from each other, showing large spatial distribution

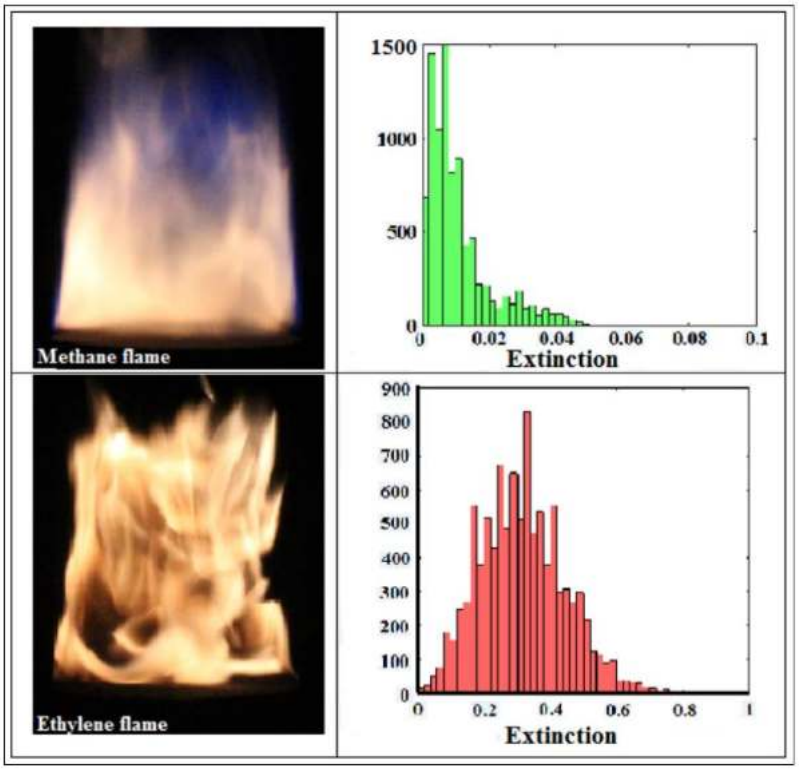

Figure 3: Comparison between methane and ethylene flames extinction histograms at 27 mm above the burner.

signal variation and maximum intensities for two studied wavelengths. Such a distribution of structures is indicative of the intermittence in the recirculation region, and is certainly the outcome of the turbulence-chemistry interactions in the bluff body wake. Only soot structures, free of PAH, are expected to be observed at the 400 nm delayed images in Fig. 4(a). The observed soot structures are thin, seemingly stretched by the instantaneous vortexes, and spatially isolated. This figures underscores that the instantaneous soot formation process does not seem occur as a spatially localized process, as found in laminar flames. However, the intermittence index distribution is highly uniform in the measurement region, $\Omega \approx 0.15$, and indicates a relatively low probability of finding soot at any given point and time. This relatively low value of Ω is the major drive behind the need of performing $4,000$ single-shot image acquisition in order to obtain meaningful statistical data.

The combined soot and PAH instantaneous signals are shown in Fig. 4(b) and (c) for the two light collection wavelengths used. Again, in this turbulent flame, the PAH and soot structures are found to randomly occur in the bluff body wake region, hindering the separation between the corresponding instantaneous signals impossible with a single camera. For this reason, the instantaneous structures shown in Fig. 4(b) and (c) may not be assigned to a single species or even to a group of species. Nevertheless, it is possible to verify that the intermittent index fields distribution is significantly different for the two used wavelengths. Indeed, for the larger wavelength, 400 nm, a nearly uniform distribution with $\Omega \approx 0.4$ is found at the lower part of the measurement region, whereas for the 340 nm detection a lobed structure is observed. Note that those Ω fields have been symmetrized around the r axis origin.

Figure 5 shows average fields of $4,000$ instantaneous images obtained for the two wavelengths of 400 and 340 nm. Note that these results are not the outcome of an image binarization process, but of a classical ensemble averaging. The discontinuity streaks in these average fields, e.g. at $z = 30$ mm, are attributed to the irregular distribution of laser sheet energy. Comparing, first, the delayed and prompt detection results of 400 nm, one may observe a rather similar spatial distribution, but with different intensities due to temporal signal decay. Again, the delay signal fields is expected to represent soot emission only, whereas the prompt signal is expected to be the combination of soot and PAH fluorescence. Figure 6 shows the distribution of the LII signal for different heights in the flame along the diameter of the burner. It's worth mentioning that the images are not symmetrized, therefore asymmetric profile of the curves is possibly due to attenuation of the beam by the soot and PAH particles present in the observed zone. This transverse profiles also show that the LII signal at the outer edges of the average flame, i.e. at = $\pm$ 30 mm are nearly independent of the flame height.

A comparison between the three detection wavelengths/delays allows to further verify the differences that exists between the results obtained. A preliminary analysis suggests that it is not possible to individualize the PAH species signal from the soot signal. However, an in-depth comparison of these measurements and averaged soot volume fraction calibration is currently being performed. Indeed, it could be possible to identify and to quantify soot volume fraction distribution

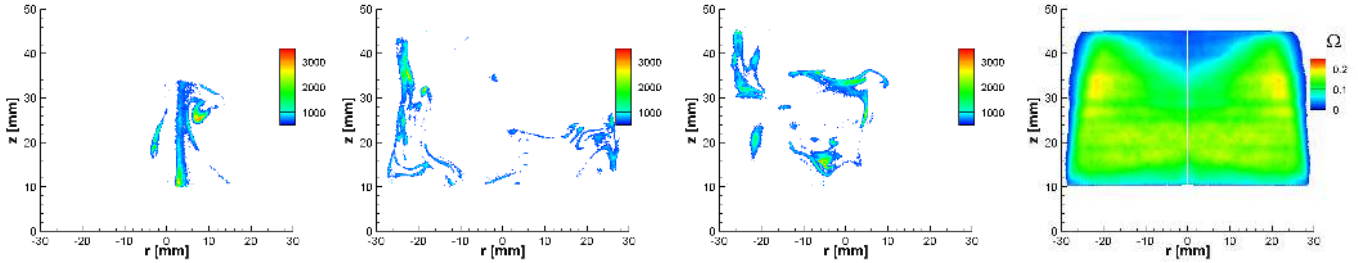

(a) Detection wavelength: 400 nm, delayed detection.

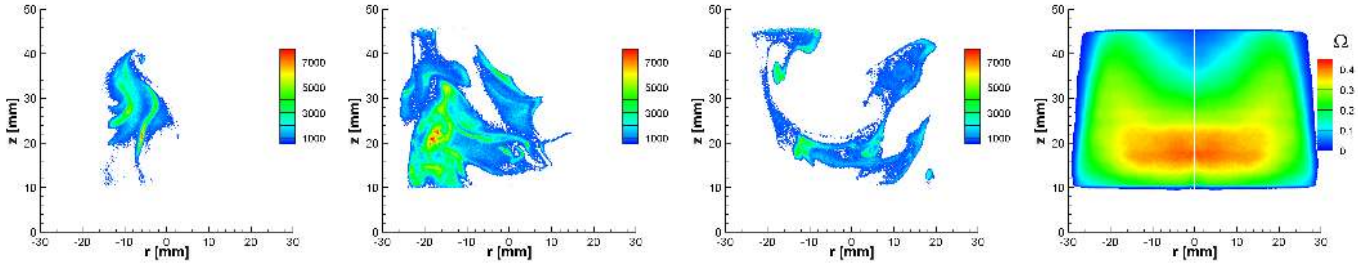

(b) Detection wavelength: 400 nm, prompt detection.

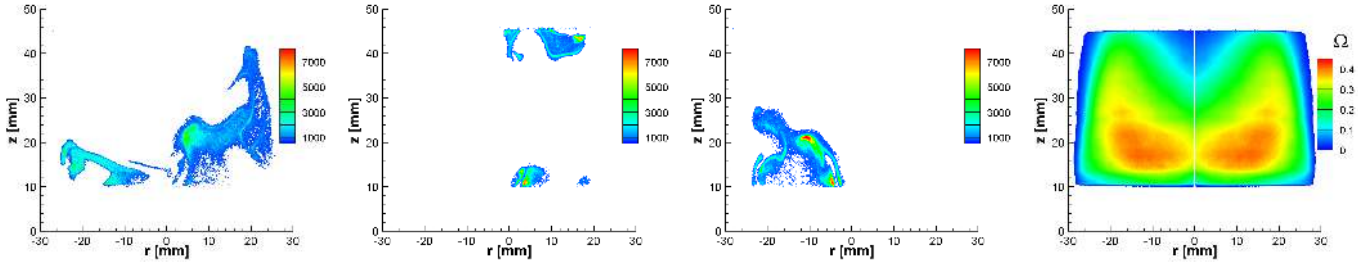

(c) Detection wavelength: 340 nm, prompt detection.

Figure 4: Fields of the instantaneous observed signals and intermittent index (Ω) distribution for the ethylene/air flame.

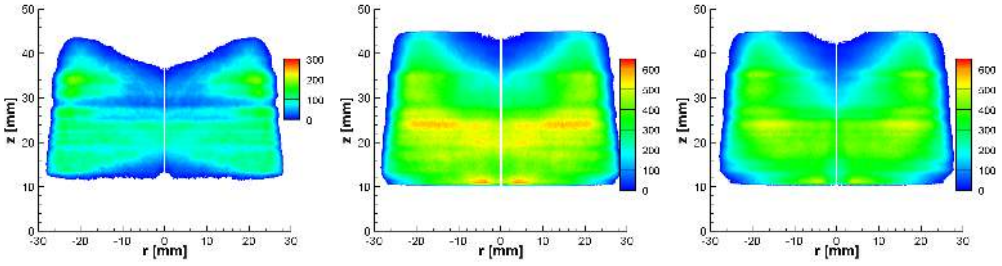

(a) Delayed detection at 400 nm. (b) Prompt detection at 400 nm. (c) Prompt detection at 340 nm.

Figure 5: Averaged measured signals for the ethylene/air flame.

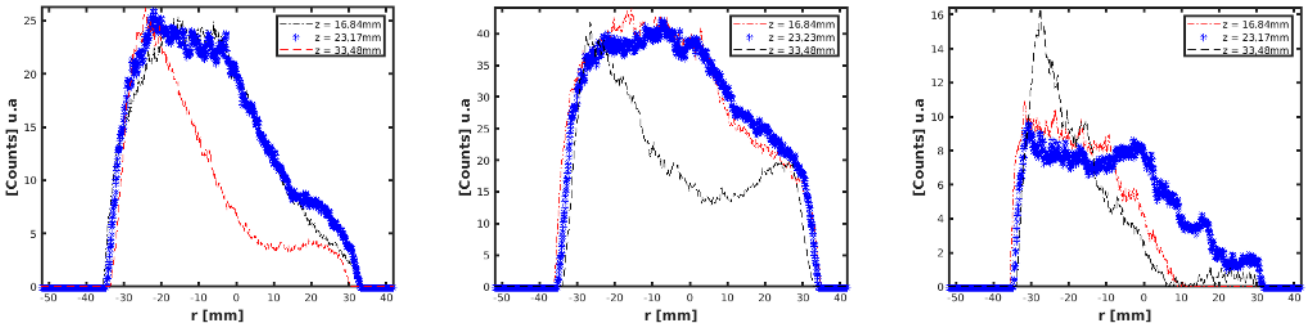

(a) Prompt detection at 340 nm. (b) Prompt detection at 400 nm. (c) Delayed detection at 400 nm.

Figure 6: Transversal distribution of soot + PAH signal for the ethylene/air flames.

and to identify the different PAH, by applying an analogy with respect to laminar flame results (Cruz Villanueva, 2018), also.

4. CONCLUSIONS AND PERSPECTIVES

- Average soot volume fraction was measured in turbulent non premixed ethylene-air and methane-air bluff body stabilized flames. Methane-air flames were characterized by an order of magnitude smaller soot concentration than the corresponding ethylene-air flames
- Soot intermittent and instantaneous soot distribution were characterized in the bluff body wake. In the studied cases, the instantaneous soot distribution indicated a large departure from the classical laminar cases, such as non-premixed stagnation point or jet.
- Future work will investigate the statistical properties of the soot incandescence field and its relationship with the turbulence properties.

5. ACKNOWLEDGEMENTS

This work was supported by Petrobras under the technical monitoring of Dr. Ricardo Serfaty (Contract 050.0080122.12.9). S. Pereira is a currently Msc CAPES scholarship student. J.J. Cruz Villanueva received a PhD scholarship from CNPq and L.F. Figueira da Silva was on leave from the Institut Pprime (CNRS, France). The authors gratefully acknowledge the support for the present research provided by Conselho Nacional de Desenvolvimento Científico e Tecnológico, CNPq, under the Research Grants No. 306069/2015-6 and 403904/2016-1.

6. REFERENCES

Axelsson, B., Collin, R. and Bengtsson, P.E., 2000. "Laser-induced incandescence for soot particle size measurements in premixed flat flames". *Applied Optics*, Vol. 39, No. 21, pp. 3683–3690.

Bourdrel, T., Bind, M.A., Béjot, Y., Morel, O. and Argacha, J.F., 2017. "Cardiovascular effects of air pollution". *Archives of Cardiovascular Diseases*, Vol. 110, No. 11, pp. 634–642.

Caetano, N. and Figueira da Silva, L.F., 2015. "A comparative experimental study of turbulent non premixed flames stabilized by a bluff-body burner". *Experimental Thermal and Fluid Science*, Vol. 63, pp. 20–33.

Chang, H. and Charalampopoulos, T.T., 1990. "Determination of the wavelength dependence of refractive indices of flame soot". *Proceedings of the Royal Society of London A: Mathematical, Physical and Engineering Sciences*, Vol. 430, No. 1880, pp. 577–591.

Chmielewski, A.G., 2013. "Nuclear power for Poland". *World Journal of Nuclear Science and Technology*, Vol. 3, pp. 123–130.

Cruz Villanueva, J.J., 2018. *Estudo experimental da distribuição de fuligem e de hidrocarbonetos aromáticos policíclicos em chamas laminares não pré-misturadas de etileno e de ar*. Ph.D. thesis, Pontiícia Universidade Católica do Rio de Janeiro.

Cruz Villanueva, J.J. and Figueira da Silva, L.F., 2016. "Study of the turbulent velocity field in the near wake of a bluff body". *Flow, Turbulence and Combustion*, Vol. 97, No. 3, pp. 715–728.

Cruz Villanueva, J.J. and Figueira da Silva, L.F., 2017. "Experimental study of laminar non premixed ethylene/air flames using laser induced incandescence and fluorescence". In *Proceedings of the 24th ABCM International Congress of Mechanical Engineering*.

Dally, B., Fletcher, D. and Masri, A., 1998a. "Flow and mixing fields of turbulent bluff-body jets and flames". *Combustion Theory and Modelling*, Vol. 2, No. 2, pp. 193–219.

Dally, B., Masri, A., Barlow, R. and Fiechtner, G., 1998b. "Instantaneous and mean compositional structure of bluff-body stabilized nonpremixed flames". *Combustion and Flame*, Vol. 114, No. 1, pp. 119–148.

Dawson, J., Gordon, R., Kariuki, J., Mastorakos, E., Masri, A. and Juddoo, M., 2011. "Visualization of blow-off events in bluff-body stabilized turbulent premixed flames". *Proceedings of the Combustion Institute*, Vol. 33, No. 1, pp. 1559 – 1566.

de Andrade Oliveira, M., Olofsson, N.E., Johnsson, J., Bladh, H., Lantz, A., Li, B., Li, Z., Aldén, M., Bengtsson, P.E., Luijten, C. and de Goey, L., 2013. "Soot, PAH and OH measurements in vaporized liquid fuel flames". *Fuel*, Vol. 112, pp. 145 – 152.

Esquiva-Dano, I., Nguyen, H.T. and Escudie, D., 2001. "Influence of a bluff-body's shape on the stabilization regime of non-premixed flames". *Combustion and Flame*, Vol. 127, No. 4, pp. 2167–2180.

Franzelli, B., Scouflaire, P. and Candel, S., 2015. "Time-resolved spatial patterns and interactions of soot, pah and oh in a turbulent diffusion flame". *Proceedings of the Combustion Institute*, Vol. 35, No. 2, pp. 1921 – 1929.

Gulder, O.L., Thomson, K.A. and Snelling, D.R., 2006. "Effect of fuel nozzle material properties on soot formation and temperature field in coflow laminar diffusion flames". *Combustion and Flame*, Vol. 144, No. 1, pp. 426–433.

Huang, R.F. and Lin, C.L., 1994. "Characteristic modes and thermal structure of nonpremixed circular-disc stabilized flames". *Combustion Science and Technology*, Vol. 100, pp. 123–139.

Lee, S.Y., Turns, S.R. and Santoro, R.J., 2009. "Measurements of soot, OH, and PAH concentrations in turbulent ethylene/air jet flames". *Combustion and Flame*, Vol. 156, No. 12, pp. 2264 – 2275.

Modest, M.F., 2013. "Chapter 1 - fundamentals of thermal radiation". In M.F. Modest, ed., *Radiative Heat Transfer (Third Edition)*, Academic Press, Boston, pp. 1 – 30. Third edition edition.

Qamar, N., Alwahabi, Z., Chan, Q., Nathan, G., Roekaerts, D. and King, K., 2009. "Soot volume fraction in a piloted turbulent jet non-premixed flame of natural gas". *Combustion and Flame*, Vol. 156, No. 7, pp. 1339 – 1347.

Quay, B., Lee, T.W., Ni, T. and Santoro, R., 1994. "Spatially resolved measurements of soot volume fraction using laser-induced incandescence". *Combustion and Flame*, Vol. 97, No. 3, pp. 384 – 392.

Sun, Y., Zwoliska, E. and Chmielewski, A.G., 2016. "Abatement technologies for high concentrations of NOx and SO_2 removal from exhaust gases: A review". *Critical Reviews in Environmental Science and Technology*, Vol. 46, No. 2, pp. 119–142.

Vander Wal, R.L., 1996. "Soot precursor material: Visualization via simultaneous LIF-LII and characterization via TEM". *Symposium (International) on Combustion*, Vol. 26, No. 2, pp. 2269 – 2275.

Vander Wal, R.L., Jensen, K.A. and Choi, M.Y., 1997. "Simultaneous laser-induced emission of soot and polycyclic aromatic hydrocarbons within a gas-jet diffusion flame". *Combustion and Flame*, Vol. 109, No. 3, pp. 399 – 414.

Zhao, H. and Ladommatos, N., 1998. "Optical diagnostics for soot and temperature measurement in diesel engines". *Progress in Energy and Combustion Science*, Vol. 24, No. 3, pp. 221 – 255.

7. RESPONSIBILITY NOTICE

The authors are the only responsible for the printed material included in this paper.